

Crystal Growth, Microhardness, Oxidation Behavior and Magnetic Properties of RMn_2Si_2 ($\text{R} = \text{La} \sim \text{Gd}$) Compounds

Shigeru OKADA*¹, Kiyokata IIZUMI*², Toetsu SHISHIDO*³, Kunio KUDOU*⁴

Abstract: RMn_2Si_2 ($\text{R} = \text{La}, \text{Ce}, \text{Pr}, \text{Nd}, \text{Sm}, \text{Gd}$) single crystals were grown from high temperature lead metal flux by slowly cooling under an argon atmosphere. The RMn_2Si_2 ($\text{R} = \text{Ce}, \text{Pr}, \text{Nd}, \text{Sm}, \text{Gd}$) crystals were obtained as thin plates with well-developed $\{001\}$ faces. The largest crystals have dimensions of approximately $2.3 \text{ mm} \times 2.3 \text{ mm} \times 0.02 \text{ mm}$. LaMn_2Si_2 was generally obtained as powder of irregular shape. The as-grown RMn_2Si_2 ($\text{R} = \text{Ce}, \text{Pr}, \text{Nd}, \text{Sm}, \text{Gd}$) crystals were used for measurements of micro-Vickers hardness at room temperature, oxidation resistance heated in air and magnetic susceptibility using a SQUID magnetometer at low temperatures. The values of the microhardness for the $\{001\}$ faces of RMn_2Si_2 are in the range of $5.8 \pm 0.4 \sim 6.5 \pm 0.5 \text{ GPa}$. The oxidation process of crystals was studied at the temperature below 1473 K by TG-DTA analyses. The TG curves show that the oxidation of CeMn_2Si_2 , PrMn_2Si_2 , NdMn_2Si_2 , SmMn_2Si_2 , GdMn_2Si_2 crystals starts at about 738, 979, 999, 784, and 763 K, respectively. Weight gains of the compounds after TG determination were measured to be in the range of 16.4 to 29.2 mass%. The results of the magnetic susceptibility measurements agree with recent previous work which has been done on these compounds.

Keywords: RMn_2Si_2 ($\text{R} = \text{La}, \text{Ce}, \text{Pr}, \text{Nd}, \text{Sm}, \text{Gd}$); Single crystal; micro-Vickers hardness; Oxidation behavior; Magnetic susceptibility

1. Introduction

RMn_2Si_2 (tetragonal, space group $I4/mmm$) crystals have attracted considerable interest because of their remarkable properties and potential application as high temperature thermoelectrics [1]. However, the data available on the properties of the RMn_2Si_2 are in most cases obtained from measurements on polycrystalline samples. Therefore, it is desirable to grow single crystals, to have more reliable information on the properties. Ternary rare earth manganese silicides have been synthesized by solid-state reaction methods and arc-melting methods [1, 2]. In Fig. 1, the crystal structure of the RMn_2Si_2 compounds with ThCr_2Si_2 -type structure is outlined. Layers of R-

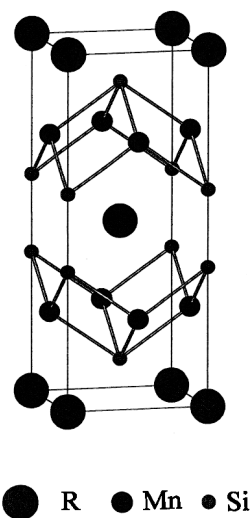


Fig. 1 Crystal structure of RMn_2Si_2 ($\text{R} = \text{rare earth}$).

*¹ 工学部都市システム工学科, 教授, 工学博士

Department of Civil and Environmental Engineering, Faculty of Engineering, Professor, Dr. of Engineering; + Corresponding author: Shigeru Okada, Tel/fax: +81-3-5481-3292, E-mail address: sokada@kokushikan.ac.jp (S. Okada).

*² 東京工芸大学, 工学部ナノ化学科, 助教授, 博士 (工学)
Faculty of Engineering, Tokyo Polytechnic University, Associate Professor, Dr. of Engineering; 1583 Iiyama, Atsugi 243-0297

*³ 東北大学, 金属材料研究所, 助教授, 工学博士
Institute for Materials Research, Tohoku University, Associate Professor, Dr. of Engineering; 2-1-1 Katahira, Aoba, Sendai 980-0812

*⁴ 神奈川大学, 工学部機械工学科, 専任講師, 博士 (工学)
Faculty of Engineering, Kanagawa University, Lecturer, Dr. of Engineering; 3-27-1 Rokkakubashi, Kanagawa, Yokohama 221-8686

atoms ($\text{R} = \text{rare earth}$) are sandwiched by infinite layers of interconnected tetragonal SiMn_4 pyramids parallel to (001) . Assuming a stoichiometric compound, Mn atoms are tetrahedrally surrounded by four Si neighbour thus being tetragonal pyramidally coordinated [3]. In the previous work, we reported the synthesis conditions of RMn_2Si_2 ($\text{R} = \text{Y}, \text{Tb}, \text{Dy}, \text{Ho}, \text{Er}, \text{Tm}, \text{Yb}, \text{Lu}$) crystals using molten lead flux, and some properties of the crystals [4-7]. In this work, we report experimental conditions for growing relatively large single crystals of RMn_2Si_2 ($\text{R} = \text{La}, \text{Ce}$,

Pr, Nd, Sm, Gd) from a high temperature lead flux in an Ar atmosphere. La, Ce, Pr, Nd, Sm and Gd are selected as rare earth elements from the light and middle region of the lanthanide series. For the single crystals so obtained, crystal morphology, crystallographic data and chemical compositions were determined, and micro-Vickers hardness, oxidation resistance heated in air and magnetic susceptibility at low temperatures of these compounds were studied.

2. Experimental

2.1. Crystal growth

The reagents used to prepare the samples were small pieces of 99.9% rare earth (La, Ce, Pr, Nd, Sm, Gd), 99.9~99.99% Mn pieces, 99.99% Si powder and 99.99% Pb pieces. The rare earth ($\text{R}=\text{La}, \text{Ce}, \text{Pr}, \text{Nd}, \text{Sm}, \text{Gd}$), Mn and Si were mixed together at atomic ratios of $\text{R}:\text{Mn}:\text{Si}=1:2:2$. The amount of Si in the starting materials was fixed at 0.4 g throughout all the experiments. Lead was added to these mixtures at a ratio of 3.8:1 in weight. Fig. 2 shows a flowchart of the syntheses process of RMn_2Si_2 crystals. The mixture of starting materials was placed in a high purity (99.9%) hBN crucible (20 mm diameter and 30 mm length) together with a hBN cover and heated in an Ar atmosphere at 1623 K for 5 h. The solution was cooled to

1073 K at a rate of 50 K h^{-1} and then quenched to room temperature. Dissolving the lead in a solution of dilute acetic acid separated the crystals.

2.2. Characterization

The crystal structures and unit cell parameters of the phases were examined by the X-ray diffraction (XRD) with monochromatic $\text{Cu K}\alpha_1$ radiation. Relatively large crystals of RMn_2Si_2 were selected under a stereomicroscope. The morphology of the crystals was examined using a four-circle diffractometer and a scanning electron microscope (SEM). The chemical composition and impurity of the crystals were analyzed with an electron probe microanalyzer (EPMA) and an energy-dispersive detector (EDX).

The micro-Vickers hardness for the crystals was measured at room temperature in air. A load of 0.49 N was applied for 15 s at about four positions on a well developed $\{001\}$ plane of each crystal. The obtained values were averaged and the experimental error was estimated.

Oxidation resistance of RMn_2Si_2 crystals was studied by TG-DTA analysis [6, 8]. Pulverized samples of about 20 mg were heated at a rate of 10 K min^{-1} in air.

Magnetic susceptibility of the powder samples of RMn_2Si_2 was measured using a commercial superconducting quantum interference device (SQUID) magnetometer in the temperature range of 2 K to 300 K.

3. Results and discussion

The XRD evidence for the crystalline phases RMn_2Si_2 obtained after reaction is shown Fig. 3. As seen from Fig. 3, for La-Mn-Si system, LaMn_2Si_2 , MnSi, Mn_5Si_3 and unknown phase were obtained, for Ce-Mn-Si system, CeMn_2Si_2 , MnSi and unknown phase were obtained, for Pr-Mn-Si system, PrMn_2Si_2 and Mn_5Si_3 were obtained, for Nd-Mn-Si and Sm-Mn-Si systems, NdMn_2Si_2 or SmMn_2Si_2 , Mn_5Si_3 and unknown phase were obtained, and for Gd-Mn-Si system, only GdMn_2Si_2 was obtained, while crystals of RMnSi (TiNiSi and PbFCl -type structures) and $\text{R}_2\text{Mn}_3\text{Si}_5$ ($\text{Sc}_2\text{Fe}_3\text{Si}_5$ -type structure) [1] were not detected by XRD. The CeMn_2Si_2 (A), PrMn_2Si_2 (B), NdMn_2Si_2 (C), SmMn_2Si_2 (D) and GdMn_2Si_2 (E) single crystals, having silver-gray and metallic luster, were generally obtained in the form of thin plates with well developed $\{001\}$ faces as shown in Fig. 4. The largest crystals have dimensions of approximately $2.3 \text{ mm} \times 2.3 \text{ mm} \times 0.02 \text{ mm}$. However, LaMn_2Si_2 was generally obtained as powder of irregular shape.

The basic crystal data and chemical compositions of RMn_2Si_2 ($\text{R}=\text{Ce}, \text{Pr}, \text{Nd}, \text{Sm}, \text{Gd}$) are listed in Table 1. The unit cell parameters of RMn_2Si_2 crystals are in relatively good agreement with previously published data ($a=0.4010(5) \text{ nm}$, $c=1.0523(5) \text{ nm}$ for CeMn_2Si_2 ; $a=0.4025 \text{ nm}$, $c=1.0555 \text{ nm}$ for PrMn_2Si_2 ; $a=0.4015(5) \text{ nm}$, $c=1.0542(5) \text{ nm}$ and $a=0.4011 \text{ nm}$, $c=1.0552 \text{ nm}$ for NdMn_2Si_2 ; $a=0.3975 \text{ nm}$, $c=1.0520 \text{ nm}$ for SmMn_2Si_2 ; $a=0.3950 \text{ nm}$, $c=1.0478$ for GdMn_2Si_2) [9]. The EDX results show that RMn_2Si_2 compounds have appreciable

Experimental

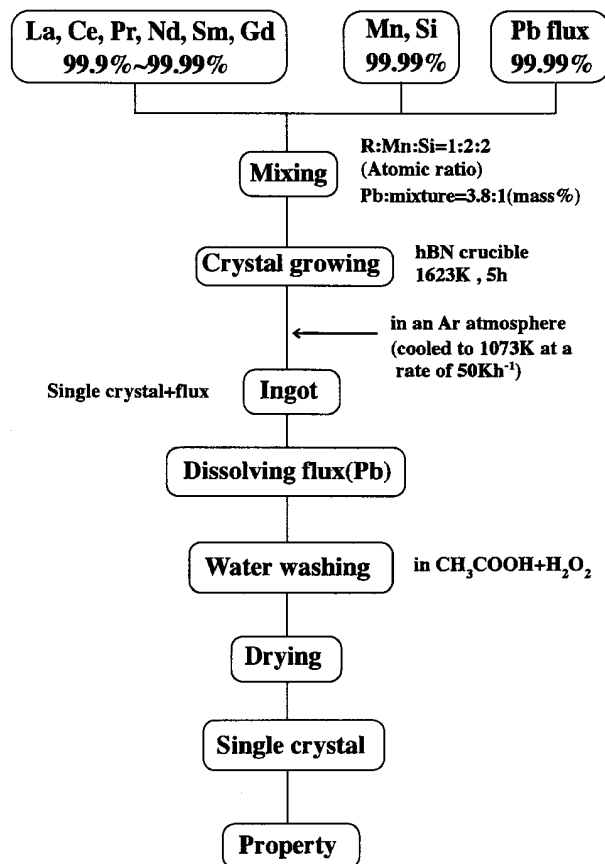


Fig. 2 Flowchart for experimental condition of RMn_2Si_2 ($\text{R}=\text{La}, \text{Ce}, \text{Pr}, \text{Nd}, \text{Sm}, \text{Gd}$) crystals.

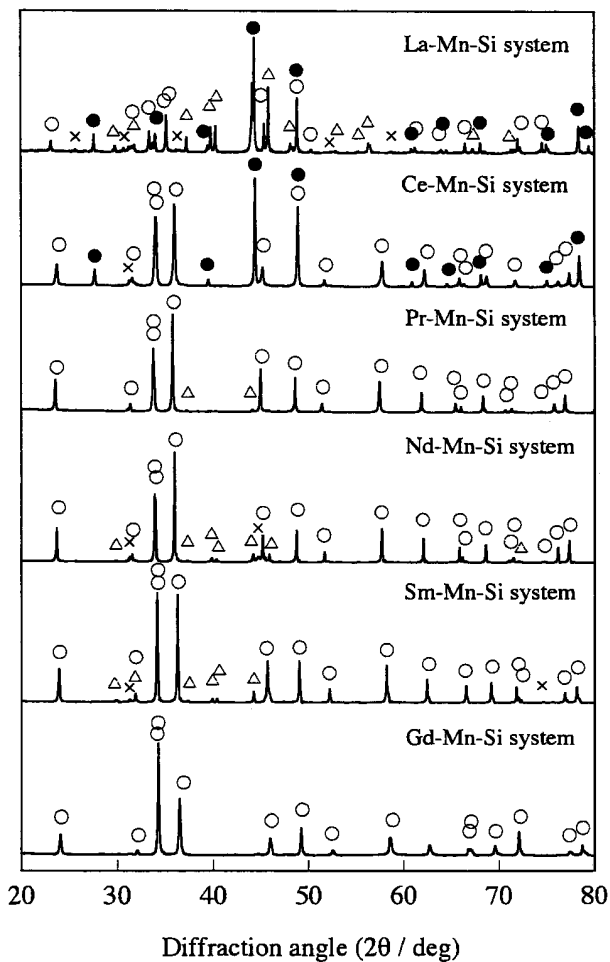


Fig. 3 Powder XRD patterns of the products obtained from R-Mn-Si (R = La, Ce, Pr, Nd, Sm, Gd) systems.
○: RMn_2Si_2 ●: MnSi △: Mn_3Si_3 ×: unknown

homogeneity ranges. No evidence has been obtained for the presence of a lead containing phase in the crystals as concluded from EPMA and EDX of RMn_2Si_2 crystals.

The values of micro-Vickers hardness for {001} faces of the as-grown crystals are listed in Table 2. The values of the microhardness for CeMn_2Si_2 , PrMn_2Si_2 , NdMn_2Si_2 , SmMn_2Si_2 and GdMn_2Si_2 are 5.8 ± 0.6 , 6.5 ± 0.5 , 6.3 ± 0.4 , 6.5 ± 0.4 and 6.8 ± 0.2 GPa, respectively. The hardness values of the RMn_2Si_2 (R = Ce, Pr, Nd, Sm, Gd) crystals were not reported in the literature earlier. These values of the RMn_2Si_2 (R = Ce, Pr, Nd, Sm, Gd) are found to be very similar to previously published data for RMn_2Si_2 (R = Er, Tm, Yb, Lu, Y) observed in the range of $5.0 \pm 0.4 \sim 7.9 \pm 0.3$ GPa [6–8].

The oxidation process of RMn_2Si_2 (R = Ce, Pr, Nd, Sm, Gd) crystals was studied below 1473 K by TG-DTA analyses, as shown in Fig. 5. The oxidation of CeMn_2Si_2 , PrMn_2Si_2 , NdMn_2Si_2 , SmMn_2Si_2 and GdMn_2Si_2 crystals began to proceed at about 738, 979, 999, 784 and 763 K,

Table 2 The values of the micro-Vickers hardness for the {001} faces of RMn_2Si_2 (R = Ce, Pr, Nd, Sm, Gd) crystals

Compound	Crystal structure	Micro-hardness (GPa)	Ref.
CeMn_2Si_2	tetragonal	5.8 ± 0.6	This work
PrMn_2Si_2	tetragonal	6.5 ± 0.5	This work
NdMn_2Si_2	tetragonal	6.3 ± 0.4	This work
SmMn_2Si_2	tetragonal	6.5 ± 0.4	This work
GdMn_2Si_2	tetragonal	6.8 ± 0.2	This work
ErMn_2Si_2	tetragonal	5.0 ± 0.4	(6)
TmMn_2Si_2	tetragonal	6.3 ± 0.3	(6)
YbMn_2Si_2	tetragonal	7.9 ± 0.3	(6)
LuMn_2Si_2	tetragonal	6.1 ± 0.4	(6)
YMn_2Si_2	tetragonal	5.6 ± 0.5	(7), (8)

Table 1 Results of the unit cell parameters and chemical analyses for RMn_2Si_2 (R = Ce, Pr, Nd, Sm, Gd) crystals

Formula unit	CeMn_2Si_2	PrMn_2Si_2	NdMn_2Si_2	SmMn_2Si_2	GdMn_2Si_2
Crystal	plate	plate	plate	plate	plate
Crystal structure	tetragonal	tetragonal	tetragonal	tetragonal	tetragonal
Space group	I4/mmm	I4/mmm	I4/mmm	I4/mmm	I4/mmm
a (nm)	0.4009(1)	0.4029(1)	0.4008(1)	0.3973(1)	0.3947(1)
c (nm)	1.0519(1)	1.0557(1)	1.0542(1)	1.0510(1)	1.0470(1)
V (nm ³)	0.1691(1)	0.1714(1)	0.1693(1)	0.1659(1)	0.1631(1)
Formula units per unit cell (Z)	2	2	2	2	2
Ce (mass%)*	44.4	—	—	—	—
Pr (mass%)*	—	44.7	—	—	—
Nd (mass%)*	—	—	45.2	—	—
Sm (mass%)*	—	—	—	47.2	—
Gd (mass%)*	—	—	—	—	47.8
Mn (mass%)*	37.4	37.4	36.3	35.1	33.6
Si (mass%)*	18.2	17.9	18.5	17.7	18.6
Chemical composition	$\text{Ce}_{1.0}\text{Mn}_{2.1}\text{Si}_2$	$\text{Pr}_{1.0}\text{Mn}_{2.1}\text{Si}_2$	$\text{Nd}_{0.9}\text{Mn}_{2.0}\text{Si}_2$	$\text{Sm}_{1.0}\text{Mn}_{2.0}\text{Si}_2$	$\text{Gd}_{0.9}\text{Mn}_{1.9}\text{Si}_2$

* EDX results.

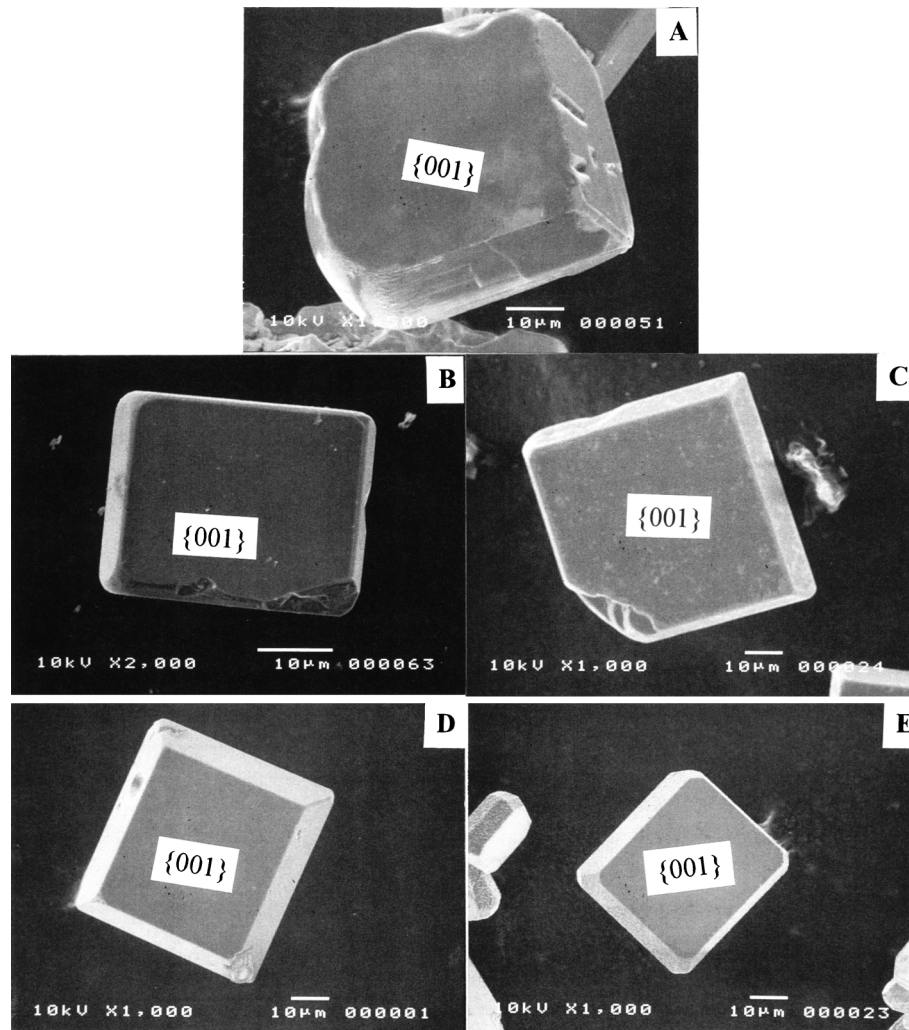


Fig. 4 SEM micrographs of RMn_2Si_2 ($\text{R}=\text{Ce}, \text{Pr}, \text{Nd}, \text{Sm}, \text{Gd}$) crystals. (A) CeMn_2Si_2 , (B) PrMn_2Si_2 , (C) NdMn_2Si_2 , (D) SmMn_2Si_2 , (E) GdMn_2Si_2

Table 3 Results of the TG/DTA measurements for RMn_2Si_2 ($\text{R}=\text{Ce}, \text{Pr}, \text{Nd}, \text{Sm}, \text{Gd}$) compounds

Compound	Oxidation start (K)	Exothermic maximum (K)	Weight gain (mass%)	Oxidation products
CeMn_2Si_2	738	1117, 1184, 1322, 1431	29.2	$\text{Ce}_4\text{Si}_3\text{O}_{12}$, MnSiO_3 , Ce_2O_3 , Mn_5Si_3 , unknown
PrMn_2Si_2	979	1200, 1305, 1366, 1444	26.8	$\text{Pr}_4\text{Si}_3\text{O}_{12}$, MnSiO_3 , Mn_5Si_3 , unknown
NdMn_2Si_2	999	1218, 1335, 1392	16.4	$\text{Nd}_4\text{Si}_3\text{O}_{12}$, Mn_5Si_3 , MnSiO_3 , unknown
SmMn_2Si_2	784	1333, 1408, 1453	19.6	$\text{Sm}_4\text{Si}_3\text{O}_{12}$, MnSiO_3 , Mn_5Si_3 , Sm_2O_3
GdMn_2Si_2	763	1213, 1270, 1402	23.9	$\text{Gd}_4\text{Si}_3\text{O}_{12}$, Gd_2O_3 , unknown

respectively. The weight gain of the compounds after heating in air up to 1473 K is 29.2, 26.8, 16.4, 19.6 and 23.9 mass%, respectively. CeMn_2Si_2 shows low oxidation resistance, while NdMn_2Si_2 show relatively high oxidation resistance. The final oxidation products were $\text{R}_4\text{Si}_3\text{O}_{12}$ ($\text{R}=\text{Ce}, \text{Pr}, \text{Nd}, \text{Sm}, \text{Gd}$), R_2O_3 ($\text{R}=\text{Ce}, \text{Sm}, \text{Gd}$), MnSiO_3 , Mn_5Si_3 [10] and an unknown phase, and so the exothermic peaks are attributed to oxidation products. The results of TG-DTA are listed in Table 3.

Magnetic characterization of the RMn_2Si_2 ($\text{R}=\text{Ce}, \text{Pr}, \text{Nd}, \text{Sm}, \text{Gd}$) samples was carried out by measuring the magnetic susceptibilities. Our results agree with recent previous work which has been done on these compounds [11–14].

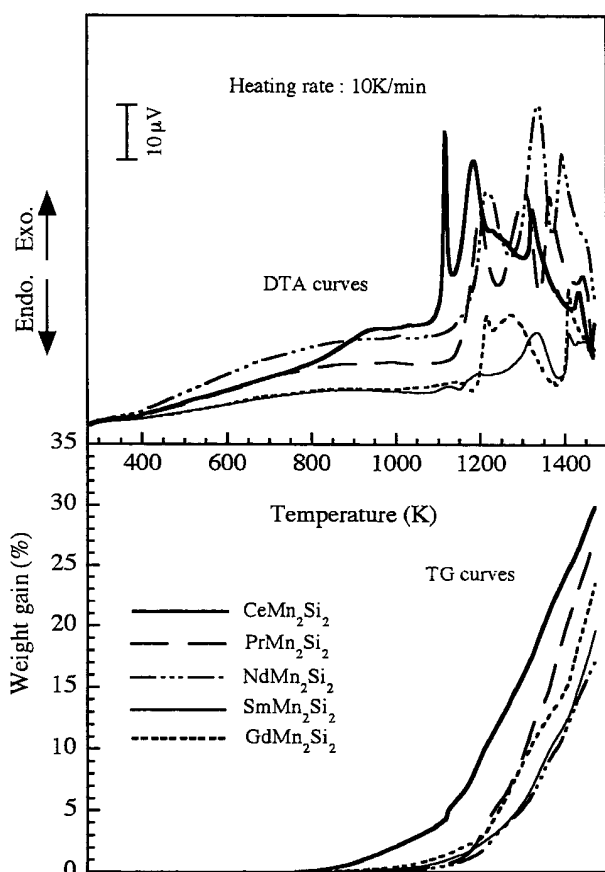


Fig. 5 TG-DTA curves of RMn_2Si_2 ($R = \text{Ce, Pr, Nd, Sm, Gd}$) crystals heated in air.

4. Conclusions

- (1) RMn_2Si_2 ($R = \text{La, Ce, Pr, Nd, Sm}$ and Gd) crystals were grown from high temperature lead metal flux by slowly cooling under an argon atmosphere at 1623 K for 5 h. The CeMn_2Si_2 , PrMn_2Si_2 , NdMn_2Si_2 , SmMn_2Si_2 and GdMn_2Si_2 single crystals were generally obtained in the form of thin plates with well developed $\{001\}$ faces. LaMn_2Si_2 was generally obtained as powder of irregular shape.
- (2) The unit cell parameters of RMn_2Si_2 ($R = \text{Ce, Pr, Nd, Sm}$ and Gd) crystals are in relatively good agreement with previously published data. The results of chemical analyses show that RMn_2Si_2 compounds have appreciable homogeneity ranges.
- (3) The values of the microhardness for the $\{001\}$ faces of RMn_2Si_2 ($R = \text{Ce, Pr, Nd, Sm}$ and Gd) are in the range of $5.8 \pm 0.4 \sim 6.5 \pm 0.5$ GPa.
- (4) The oxidation process of crystals was studied at the temperature below 1473 K by TG-DTA analyses. The TG curves show that the oxidation of CeMn_2Si_2 , PrMn_2Si_2 , NdMn_2Si_2 , SmMn_2Si_2 , GdMn_2Si_2 crystals

starts at about 738, 979, 999, 784, and 763 K, respectively. Weight gains of the compounds after TG determination were measured to be in the range of 16.4 to 29.2 mass%.

- (5) The results of the magnetic susceptibility measurements agree with recent previous work which has been done on these compounds.

Acknowledgements

This study was performed under the Interuniversity Cooperative Research Program of the Laboratory for Advanced Materials (LAM), Institute for Materials Research (IMR), Tohoku University. The authors would like thank to Prof. Dr. M. Ogawa and Miss N. Suzuki of Tokyo Polytechnic University for their help in the experiments.

References

- [1] E. Parthé, B. Chabot, in: K. A. Gschneidner Jr., L. Eyring (Eds.), Handbook of Physics and Chemistry of Rare Earths, Vol. 6, North-Holland, Amsterdam, 1984, p. 212.
- [2] K. S. V. Narasimhan, V. Us Rao, W. E. Wallace, AIP Conf. Proc. 29 (1976) 594.
- [3] A. Grytsiv, A. L-Jasper, H. Flandorfer, P. Rogl, K. Hiebl, C. Godart, T. Velikanova, J. Alloys Compd. **266** (1998) 7.
- [4] S. Okada, M. Ogawa, T. Shishido, K. Iizumi, K. Kudou, H. Kanari, K. Nakajima, P. Rogl, J. Crystal Growth **236** (2002) 617.
- [5] S. Okada, K. Kudou, T. Mori, K. Iizumi, T. Shishido, T. Tanaka, K. Nakajima, P. Rogl, Jpn. J. Appl. Phys. **41** (2002) L555.
- [6] S. Okada, K. Kudou, T. Mori, K. Iizumi, T. Shishido, T. Tanaka, P. Rogl, J. Crystal Growth **244** (2002) 267.
- [7] S. Okada, K. Kudou, T. Mori, K. Iizumi, T. Shishido, T. Tanaka, P. Rogl, Bulletin of Science and Engineering Research Institute, Kokushikan University, No. 15, March, (2003) 23.
- [8] K. Kudou, S. Okada, T. Mori, K. Iizumi, T. Shishido, T. Tanaka, H. Kanari, P. Rogl, J. Alloys Compd. **358** (2003) 182.
- [9] P. Rogl, in: K. A. Gschneidner Jr., L. Eyring (Eds.), Handbook of Physics and Chemistry of Rare Earths, Vol. 7, North-Holland, Amsterdam, 1984, p.26.
- [10] S. Okada, T. Shishido, Y. Ishizawa, M. Ogawa, K. Kudou, T. Fukuda, T. Lundström, J. Alloys Compd. **317-318** (2001) 315.
- [11] A. Szytula, J. Leciejewicz, in: K. A. Gschneidner Jr., L. Eyring (Eds.), Handbook on the Physics and Chemistry of Rare Earths, Vol. 12, North-Holland, Amsterdam, 1989, p.133.
- [12] R. Welter, G. Venturini, D. Fruchart, B. Malaman, J. Alloys Compd. **191** (1993) 263.
- [13] I. Nowik, Y. Levi, I. Felner, E. R. Bauminger, J. Magn. Mater. **47** (1995) 373.
- [14] S. Okada, K. Iizumi, T. Mori, T. Shishido, K. Kudou, T. Tanaka, P. Rogl, T. Lundström, J. Alloys Compd. **383** (2004) 254.